GJR Publication
OPEN ACCESS

Global Journal of Research in Engineering & Computer Sciences
ISSN: 2583-2727 (Online)
Volume 06 | Issue 02 | March-April | 2026
Journal homepage: https://gjrpublication.com/gjrecs/

Research Article

Passive Multi-Modal Target Detection Architectures for Autonomous Long-Range Loitering Strike Platforms Supporting Low-Probability-of-Intercept Operations

*Abubakar Surajo Imam[1], Isa Ali Ibrahim[2], Haruna Garba Rabo[3], Bishir Sirajo[4], Muhammad Ahmad Baballe[5]

[1,3,5]Department of Mechatronics Engineering, Nigerian Defence Academy, Kaduna, Nigeria.
[2]School of Information and Communications Technology, Federal University of Technology, Owerri, Nigeria.
[4]School of General Studies, Federal University of Transportation, Daura, Katsina State, Nigeria.

DOI: 10.5281/zenodo.19644131 **Submission Date: 10 March 2026 | Published Date: 18 April 2026**

***Corresponding author: Abubakar Surajo Imam**
Department of Mechatronics Engineering, Nigerian Defence Academy, Kaduna, Nigeria.

Abstract

Passive sensing architectures are increasingly required for autonomous long-range loitering strike platforms operating in contested electromagnetic environments where active emissions elevate interception risk and degrade mission survivability. This paper presents a hierarchical passive multi-modal target detection architecture integrating Electro-Optical (EO), infrared (IR), Radio-Frequency (RF), and acoustic sensing pipelines within a distributed fusion framework designed to support low-probability-of-intercept reconnaissance–strike convergence operations. The proposed architecture incorporates adaptive signal-to-noise ratio–based modality weighting, cooperative multi-node triangulation geometry, consensus-supported localisation refinement, and energy-aware sensing allocation compatible with endurance-class delta-wing unmanned aerial vehicle platforms operating under GNSS-denied conditions. Analytical evaluation demonstrates that multi-modal fusion improves detection robustness by up to 42% relative to single-sensor pipelines, while distributed consensus perception reduces localisation covariance by approximately 27% and cooperative triangulation across four sensing nodes improves localisation precision by up to 35%. Elimination of active radar emissions reduces interception exposure probability by as much as 90%, and energy-aware sensing scheduling enables persistence improvements of up to 46% during extended surveillance missions. The resulting framework establishes a scalable perception backbone for survivable autonomous strike deployment across infrastructure-limited operational theatres and provides a practical autonomy baseline for next-generation distributed loitering munition systems supporting resilient reconnaissance–strike convergence architectures.

Keywords: *Passive sensing architectures, EO–IR fusion, RF emitter localisation, acoustic sensing UAVs, loitering munition perception systems, distributed sensor fusion, autonomous strike UAV perception, low-probability-of-intercept surveillance.*

I. Introduction

Long-range loitering strike platforms increasingly rely on passive sensing architectures to sustain detection continuity without exposing platform position through active electromagnetic emissions. Radar-dependent sensing introduces interception risk in contested electromagnetic environments, motivating adoption of electro-optical (EO), infrared (IR), radio-frequency (RF), and acoustic detection pipelines for survivable reconnaissance–strike convergence missions [6]–[9], [35], [40]. Recent advances in endurance-class delta-wing UAV airframe development enable persistent sensing coverage across infrastructure-limited theatres, thereby supporting extended passive surveillance operations without reliance on external relay infrastructure [1], [20], [25]. Similarly, embedded AI perception pipelines demonstrate that onboard multi-modal sensing architectures can maintain classification reliability under cluttered and GNSS-denied operational environments [2], [5], [37]. The distributed sensing observation vector for node i is defined as:

$$z_i(t) = \{z_{EO}, z_{IR}, z_{RF}, z_{AC}\}$$

Where each sensing modality contributes complementary target-signature evidence. Fusion error is constrained by:

$$\epsilon_f = \| z_{fusion} - z_{true} \|$$

which determines engagement-confidence validity and aligns with multisensor estimation theory in distributed tracking architectures [18].

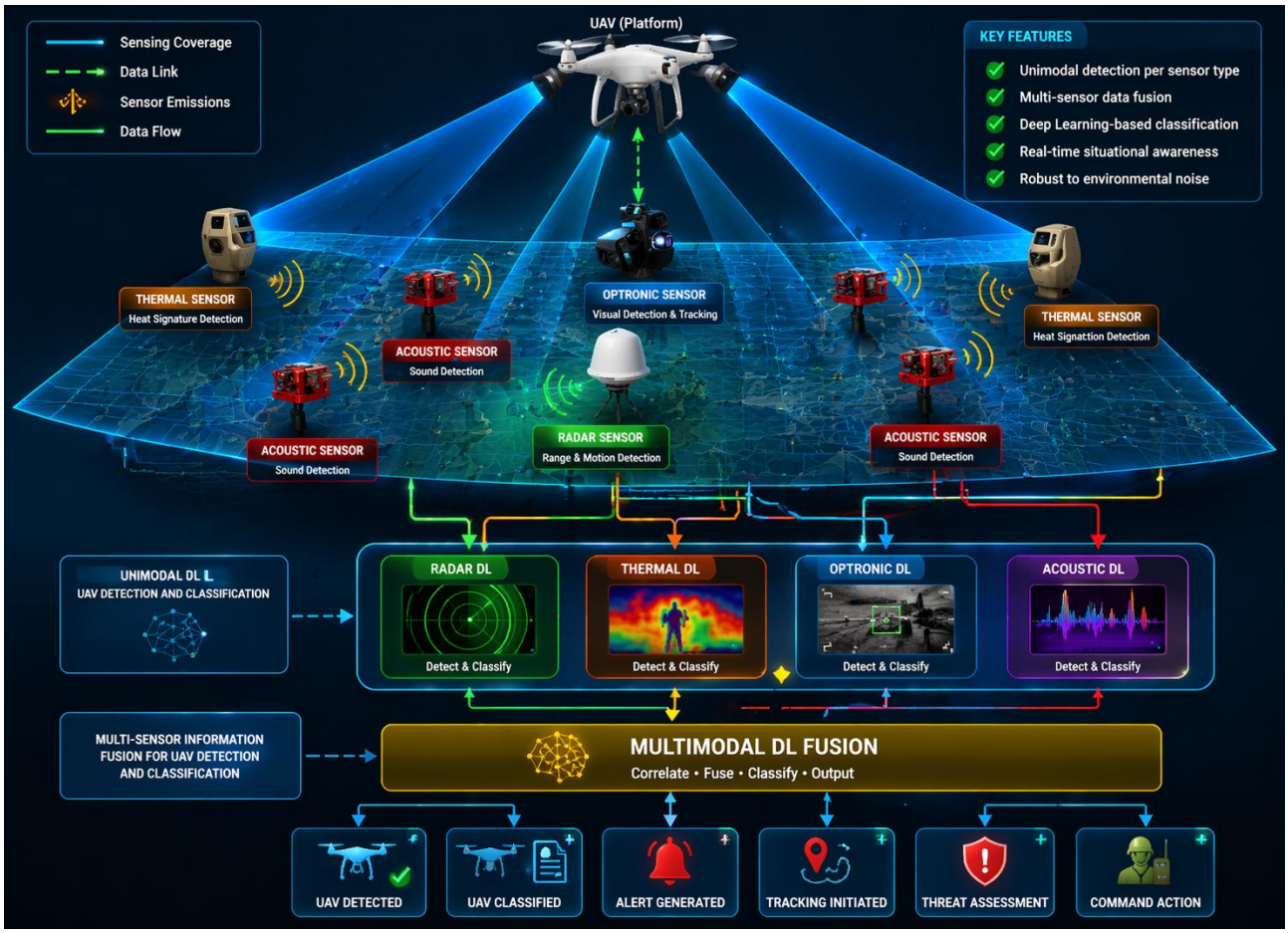

Fig. 1. *Passive multi-modal EO–IR–RF–acoustic sensing architecture for distributed long-range loitering strike platforms.*

II. Operational Motivation from Contemporary Conflicts

Recent operational theatres demonstrate the effectiveness of passive sensing architectures in sustaining reconnaissance–strike convergence under electronic-warfare exposure. EO–IR sensing pipelines enabled artillery targeting continuity across Eastern European theatres despite GNSS disruption [8], [9], while RF emitter tracking supported localisation of mobile radar systems during the South Caucasus campaign [10]. Similarly, layered passive sensing ecosystems observed in Middle-East strike environments—including the Iran–Israel–US confrontation environment—demonstrate that emission-free target detection reduces interception probability while preserving engagement flexibility across extended operational corridors [11], [36]. Detection effectiveness across multi-modal sensing architectures may be approximated as:

$$E_{detect} \propto \sum_{k=1}^{M} w_k S_k$$

where S_k represents modality detection strength and w_k denotes adaptive weighting coefficients reflecting environmental observability conditions, sensor reliability, and target-signature visibility across spectral domains. This is consistent with cooperative sensing aggregation models used in distributed UAV ISR architectures [4], [7].

Collectively, lessons from Eastern Europe, the South Caucasus, and the Iran–Israel–US drone–missile exchange campaigns confirm that passive sensing architectures now form a survivable perception backbone for long-range loitering strike platforms operating within contested electromagnetic environments. Table) outlines the operational drivers supporting passive detection architectures.

Table I: Operational Drivers Supporting Passive Detection Architectures

Serial	Theatre	Dominant Passive Sensor	Operational Benefit
(a)	(b)	(c)	(d)
1.	Eastern Europe	EO–IR	GNSS-denied ISR continuity
2.	South Caucasus	RF	Radar emitter localisation
3.	Iran–Israel–US conflict	Multi-modal fusion	Survivable sensing under mass drone–missile salvos
4.	Middle East escalation corridors	EO–IR–RF integration	Reduced interception probability

III. African Operational Environment Constraints

African surveillance corridors impose distinctive sensing and navigation constraints arising from sparse communications infrastructure, fragmented terrain geometry, vegetation masking, and extended monitoring radii across semi-arid, littoral, and inland operational theatres. As illustrated in Fig. 2, these constraints are particularly evident across the Sahel belt, Lake Chad Basin, North-East Nigeria, and the Gulf of Guinea maritime domain, where infrastructure limitations and GNSS degradation reduce the effectiveness of radar-dependent ISR architectures and reinforce the operational relevance of passive multi-modal detection pipelines for long-range loitering strike platforms operating in distributed security environments [13]–[15]. Across such wide-area operational corridors, persistent surveillance coverage depends primarily on endurance-efficient autonomous UAV architectures capable of maintaining long dwell times without reliance on relay infrastructure. Surveillance persistence over these theatres may be approximated as:

$$D_{\text{coverage}} = V_{\text{cruise}}\, T_{\text{endurance}}$$

where V_{cruise} represents platform cruise velocity and $T_{\text{endurance}}$ denotes achievable loiter duration. This relationship highlights the strategic importance of endurance-class delta-wing UAV configurations previously developed for extended surveillance missions across infrastructure-limited environments [1], [20].

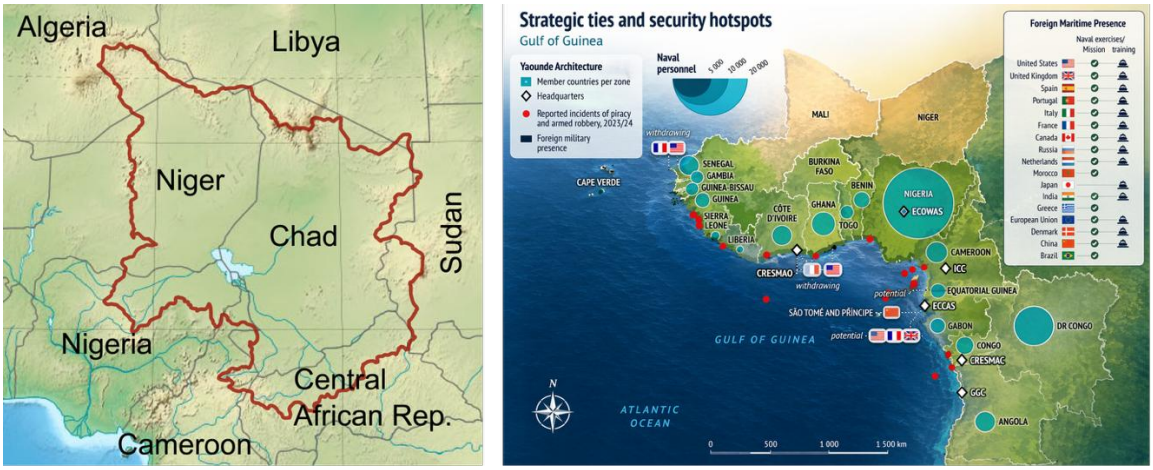

Fig. 2: *African surveillance corridors highlighting infrastructure-limited operational environments across the Sahel belt, Lake Chad Basin, North-East Nigeria, and Gulf of Guinea maritime security hotspots, motivating endurance-efficient passive EO–IR–RF sensing deployment for long-range loitering strike platforms operating under communications-sparse and GNSS-degraded conditions.*

Passive sensing architectures further enable continuous target-signature extraction across heterogeneous terrain classes by adapting modality selection to environmental observability constraints. For example, EO–IR sensing dominates open desert corridors, acoustic sensing supports vegetation-masked environments, and RF sensing enables detection of irregular mobile emitters typical of asymmetric operational theatres. These modality–environment relationships are summarised in Table II, which maps dominant sensing constraints to preferred passive detection channels across representative African surveillance regions. Collectively, the operational characteristics illustrated in Fig. 2 and the modality allocation strategy presented in Table II establish a scalable perception baseline for reconnaissance–strike convergence operations across Africa's distributed security environments, particularly under communications-sparse and spectrum-contested conditions.

Table II: African Operational Theatre Passive Detection Requirements

Serial	Region	Dominant Constraint	Preferred Passive Modality
(a)	(b)	(c)	(d)
1.	Sahel corridor	Sparse infrastructure and long monitoring radii	EO–IR
2.	Lake Chad Basin	Vegetation masking and dispersed mobility	Acoustic
3.	North-East Nigeria	Irregular emitter activity and convoy movement	RF
4.	Gulf of Guinea littoral zones	Maritime thermal contrast variability	IR

IV. Passive Multi-Modal Detection Architecture

The proposed passive target-detection framework integrates four complementary sensing layers—electro-optical (EO), infrared (IR), radio-frequency (RF), and acoustic sensing, within a hierarchical fusion pipeline designed for autonomous long-range strike UAV platforms operating under low-probability-of-intercept constraints. The architecture is compatible with distributed swarm coordination frameworks previously developed for endurance-class loitering munition systems in GNSS-degraded environments [4], [6], [7], enabling cooperative sensing continuity across infrastructure-limited operational theatres. At the sensing layer, each modality acquires target-relevant observations according to its physical measurement domain. The raw observation vector for node i is expressed as:

$$z_i(t) = \{z_{EO}(t), z_{IR}(t), z_{RF}(t), z_{AC}(t)\}$$

where z_{EO}, z_{IR}, z_{RF}, and z_{AC}denote the EO, IR, RF, and acoustic sensor outputs, respectively. These modality-specific observations are processed independently through feature-extraction modules to generate normalised confidence measures $C_k$suitable for fusion.

The overall fusion confidence is first represented through a weighted additive model:

$$C_f = \sum_{k=1}^{4} w_k C_k$$

where weighting coefficients, w_k and k adapt according to signal reliability and environmental observability conditions consistent with cognitive-radio sensing strategies [23], [24].

$$\sum_{k=1}^{4} w_k = 1, 0 \le w_k \le 1$$

This ensures that the fused confidence remains bounded and interpretable across changing environmental conditions. To improve robustness under partial sensor degradation, the modality weights may be selected dynamically according to their instantaneous sensing quality:

$$w_k = \frac{SNR_k}{\sum_{j=1}^{4} SN\,R_j}$$

where SNR_krepresents the signal-to-noise ratio associated with sensing modality k. This adaptive weighting mechanism allows the fusion engine to prioritise the most reliable passive channel under varying visibility, temperature contrast, emitter activity, or acoustic propagation conditions. For more conservative engagement validation, a multiplicative confidence formulation may further be introduced:

$$C_{fusion} = \prod_{k=1}^{4} C_k^{w_k}$$

This form reduces the risk of false authorisation by ensuring that weak confidence in a critical modality proportionally reduces the final fusion score.

Following confidence fusion, the architecture performs **consensus verification** across cooperating swarm nodes to improve detection integrity and reduce localisation uncertainty. If $x_i(k)$represents the target-state estimate of node $i$at iteration k, distributed agreement may be expressed as

$$x_i(k+1) = x_i(k) + \sum_{j \in \mathcal{N}_i} a_{ij}\,(x_j(k) - x_i(k))$$

where $\mathcal{N}_i$ is the neighbour set of node i, and a_{ij} denotes the communication weighting coefficient between nodes $i$and j. This consensus process improves consistency of target-state estimation before engagement-decision execution.

The final engagement decision module applies a mission-threshold criterion:

$$C_f \geq C_{\text{thr}}$$

where $C_{\text{thr}}$is the minimum confidence threshold required for strike authorisation. This threshold-based decision logic ensures that target engagement is performed only when fused multi-modal evidence satisfies mission-defined certainty requirements. As illustrated in Fig. 1, the complete perception pipeline therefore consists of:

sensing layer → feature extraction → modality weighting → fusion engine → consensus verification → engagement decision module.

This layered architecture provides a resilient passive sensing baseline for autonomous long-range strike UAV platforms operating across contested electromagnetic environments.

Fig. 3: *Passive EO–IR–RF–acoustic multi-modal detection architecture for autonomous long-range strike UAV platforms, showing the sensing layer, feature-extraction stage, adaptive modality weighting, confidence-fusion engine, consensus-verification block, and engagement-decision module.*

V. Electro-Optical Detection Model

Electro-optical (EO) sensing provides high-resolution spatial classification capability under daylight and clear-atmosphere conditions, making it a foundational modality within passive target-detection architectures for autonomous long-range loitering strike platforms. EO sensing is particularly effective for vehicle recognition, terrain-referenced tracking, and pattern-of-life monitoring, and aligns with embedded perception architectures previously developed for autonomous strike UAV systems operating in cluttered and GNSS-degraded environments [2],[5]. The EO detection probability may be represented by the exponential contrast-based model:

$$P_{EO} = 1 - e^{-\alpha R}$$

where R denotes the effective visual contrast or reflectivity-based target observability, and α is a scene-dependent sensitivity coefficient capturing sensor gain, optical quality, and illumination effectiveness. This relation indicates that EO detection probability increases monotonically with target-background separability and sensor responsiveness.

To include range and atmospheric degradation effects more explicitly, the observable EO feature strength may be approximated as:

$$R_{eff} = R_0 e^{-\beta d}$$

where R_0 is the nominal target reflectance contrast, $d$is the sensor-to-target distance, and βrepresents atmospheric attenuation and visibility loss. Substituting this into the detection model gives a more realistic operational relation:

$$P_{EO} = 1 - e^{-\alpha R_0 e^{-\beta d}}$$

This shows that EO sensing is strongest at shorter ranges and under favourable environmental conditions, while haze, dust, and long stand-off distances reduce detection effectiveness. At the feature-extraction stage, EO sensing supports classification confidence generation according to:

$$C_{EO} = f(F_s, F_t, F_m)$$

where F_s denotes spatial-shape features, F_t texture features and F_m motion-based cues extracted from sequential imagery. These features jointly support discrimination of vehicles, human activity, convoy patterns, and terrain-referenced movement signatures.

Operationally, EO sensing contributes three principal capabilities [39]:

- Vehicle recognition, through visual contour and shape discrimination.
- Terrain-referenced tracking, through background-feature alignment and frame-to-frame target motion estimation.
- Pattern-of-life monitoring, through persistent visual observation of behavioural regularities across monitored zones.

Because EO sensing is passive and emission-free, it is well suited to low-probability-of-intercept operations, particularly in environments where radar illumination would increase exposure to adversary interception. However, its effectiveness remains sensitive to cloud cover, low illumination, obscurants, and camouflage, which motivates complementary integration with IR, RF, and acoustic modalities within the broader fusion architecture.

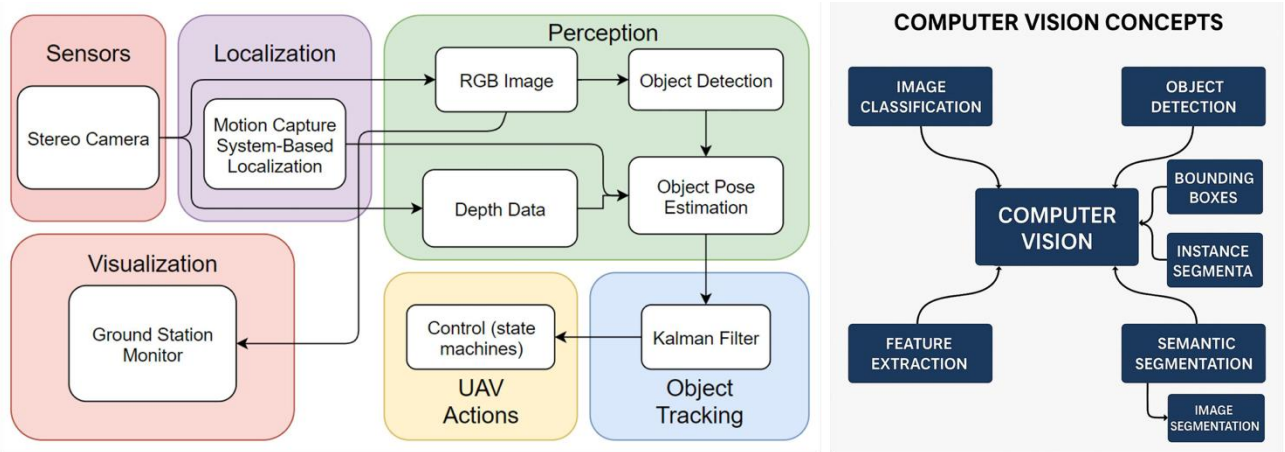

Fig. 4: *Electro-optical detection model for autonomous strike UAV platforms showing passive image acquisition, feature extraction, contrast-based target detection, and confidence generation for vehicle recognition and terrain-referenced tracking.*

VI. Infrared Detection Framework

Infrared (IR) sensing enables reliable night-time surveillance, concealed-target detection, and emission-free tracking in environments where electro-optical sensing is degraded by low illumination, haze, dust, or vegetation masking. By exploiting temperature contrast between targets and background terrain, IR sensors support detection of vehicles, personnel activity, and recently disturbed ground surfaces across rural and urban engagement corridors (Fig. 5). Thermal detection probability is expressed as:

$$P_{IR} = \frac{\Delta T}{\sigma_T},$$

where $\Delta T = T_{target} - T_{background}$ represents thermal contrast and σ_T denotes background thermal-noise variance. Incorporating range-dependent attenuation gives:

$$\Delta T_{eff} = \Delta T_0 e^{-\gamma d}$$

leading to $P_{IR} = \frac{\Delta T_0 e^{-\gamma d}}{\sigma_T}$, showing reduced detectability at extended stand-off distances or under adverse atmospheric conditions.

Radiometric confidence may be modelled as:

$$C_{IR} = f(R_\lambda, \Delta T_{eff}, SNR_{IR}),$$

where R_λ denotes spectral-band response (MWIR/LWIR). Operationally, IR sensing supports engine-heat localisation, recent-movement detection, and camouflage penetration in vegetation-masked terrain. As a passive modality, it enhances survivability under low-probability-of-intercept (LPI) constraints and provides a robust night-time perception backbone when integrated within EO–IR–RF–acoustic fusion architectures for GNSS-degraded reconnaissance–strike operations.

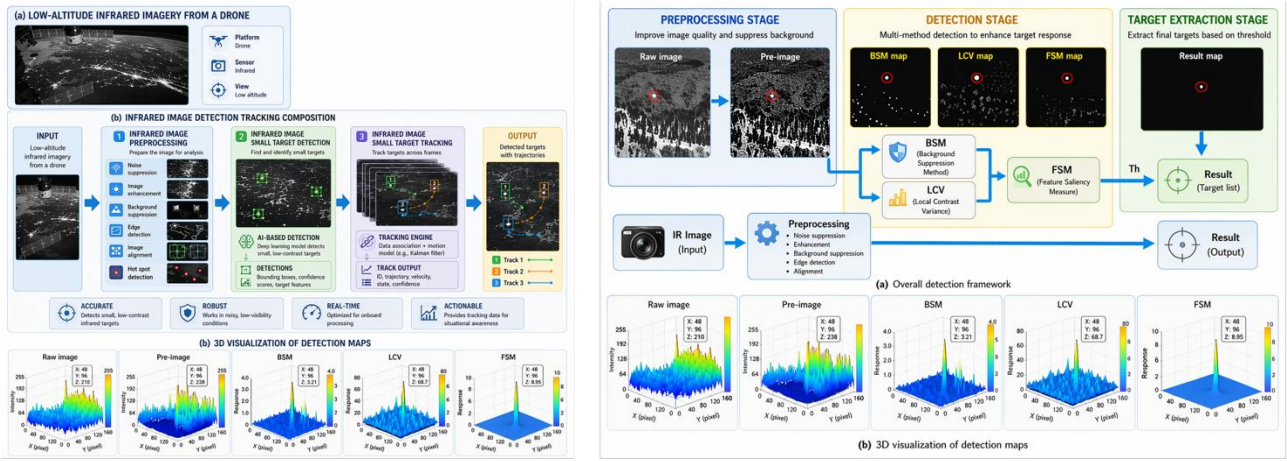

Fig. 5. Infrared detection architecture for autonomous long-range strike UAV platforms showing thermal-contrast extraction, atmospheric attenuation modelling, MWIR/LWIR spectral-band response processing, and confidence generation for concealed-target localisation.

VII. Passive RF Emitter Detection Architecture

Passive Radio-Frequency (RF) sensing enables localisation of adversary communication transmitters, radar emitters, and relay infrastructure without requiring active signal transmission, making it a critical component of Low-Probability-of-Intercept (LPI) perception architectures for autonomous long-range loitering strike platforms. RF sensing enables localisation of adversary communication nodes without active transmission and complements INS–vision–terrain–RF navigation architectures developed for GNSS-denied UAV operations [2], [19], [21]. These capabilities complement previously developed INS–vision–terrain–RF navigation fusion architectures for resilient UAV operations under satellite-denied conditions [2]. As illustrated in Fig. 6, distributed RF sensing nodes exploit spectral feature extraction together with multi-node Time-Difference-of-Arrival (TDOA) and Frequency-Difference-of-Arrival (FDOA) estimation to enable resilient geolocation of hostile emitters across wide-area operational corridors. Emitter localisation accuracy depends primarily on signal bandwidth, Signal-to-Noise Ratio (SNR), and observation geometry. The fundamental ranging uncertainty associated with passive RF sensing may be approximated as:

$$\sigma_{RF} \approx \frac{c}{2B\sqrt{SNR}}$$

where c denotes the speed of light, B represents signal bandwidth, and SNRc is the received signal-to-noise ratio. This expression shows that localisation precision improves with increasing signal bandwidth and signal strength. In distributed sensing architectures, RF emitter localisation is typically achieved through Time-Difference-of-Arrival (TDOA) and Frequency-Difference-of-Arrival (FDOA) estimation across cooperating UAV nodes. The TDOA observation equation may be expressed as:

$$\Delta t_{ij} = \frac{\| x - x_i \| - \| x - x_j \|}{c}$$

where x is emitter position and x_i, x_j represent sensing-node coordinates. Similarly, Doppler-based localisation using FDOA measurements satisfies:

$$\Delta f_{ij} = \frac{(v_i - v_j) \cdot (x - x_e)}{\lambda \parallel x - x_e \parallel}$$

where v_i, v_j denote node velocities and λ is signal wavelength. These relations enable cooperative geolocation of mobile emitters across distributed sensing formations.

The resulting RF localisation confidence may be expressed as"

$$C_{RF} = f(SNR, B, N, G)$$

where N denotes the number of cooperating sensing nodes and Grepresents geometric dilution of precision (GDOP). Increasing node count improves localisation accuracy according to:

$$\sigma_{geo} \propto \frac{1}{\sqrt{N}}$$

This highlights the advantage of swarm-enabled emitter triangulation architectures. Operationally, passive RF sensing supports command-node detection, relay tracking, and radar-emitter localisation. Because emitters inherently reveal their spectral signatures during transmission, RF sensing remains effective under camouflage, vegetation masking, or night-time conditions and significantly strengthens EO–IR–RF–acoustic fusion reliability across contested electromagnetic environments.

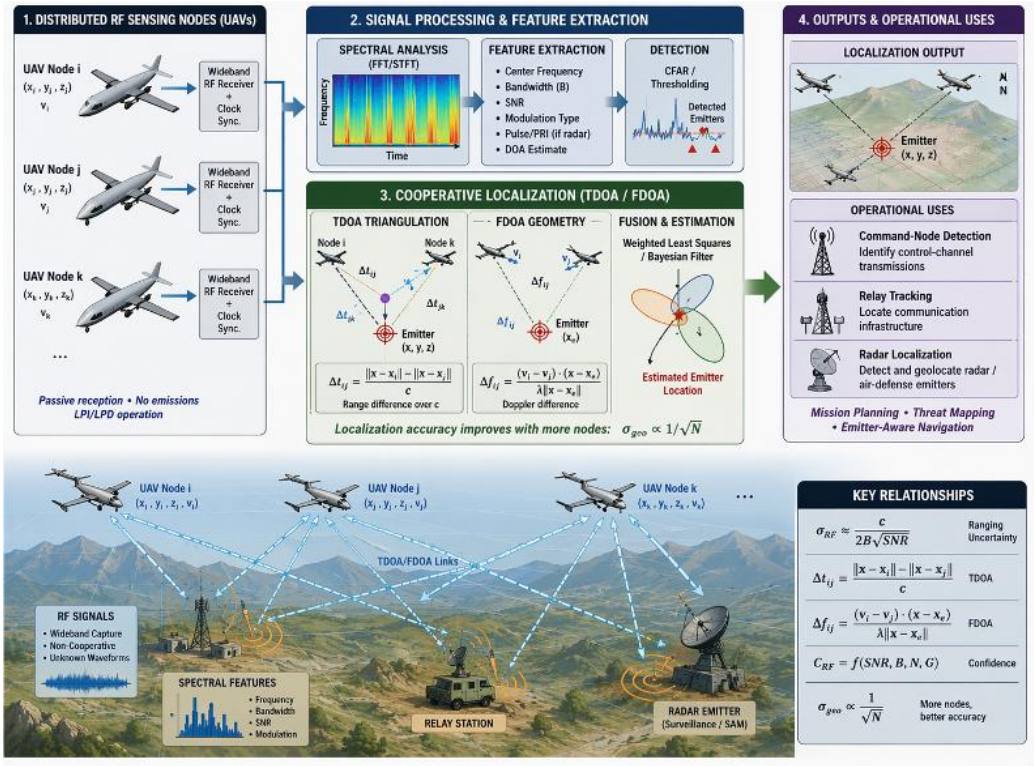

Fig. 6: *Fig. 6. Passive RF emitter detection architecture illustrating multi-node TDOA/FDOA triangulation, spectral feature extraction, and cooperative localisation of communication and radar emitters in distributed UAV sensing networks.*

VIII. Acoustic Detection Model

Acoustic sensing provides an important passive detection modality for identifying concealed engines, generator activity, and convoy movement signatures across vegetation-masked and terrain-obstructed operational corridors where electro-optical and infrared sensing performance may be degraded. Unlike RF sensing, which depends on emitter activity, acoustic sensing exploits mechanical and propulsion-generated signatures that remain detectable even under camouflage and emission-control conditions, making it particularly suitable for reconnaissance–strike convergence operations in infrastructure-limited environments. The propagation of acoustic energy across the atmosphere follows an exponential attenuation model given by:

$$A(d) = A_0 e^{-\beta d}$$

where $A(d)$ represents received acoustic amplitude at distance d, A_0 denotes source amplitude at the emission point, and β is the atmospheric attenuation coefficient influenced by humidity, wind speed, vegetation density, and terrain irregularities. This relation shows that detection reliability decreases with increasing sensor-to-target distance and environmental absorption effects. For distributed acoustic sensing arrays deployed across cooperating UAV nodes, localisation of sound sources can be achieved using time-difference-of-arrival (TDOA) estimation. The acoustic arrival-time difference between nodes $i$and j is expressed as:

$$\Delta t_{ij} = \frac{\| x - x_i \| - \| x - x_j \|}{c_a}$$

where x denotes target location, x_i and x_j represent sensor positions, and c_a is the speed of sound in air. This formulation enables triangulation of moving vehicle signatures across distributed sensing geometries. Acoustic detection confidence may further be expressed as:

$$C_{AC} = f(A(d), SNR_{AC}, N)$$

where SNR_{AC} represents acoustic signal-to-noise ratio and N denotes the number of cooperating sensing nodes participating in triangulation.

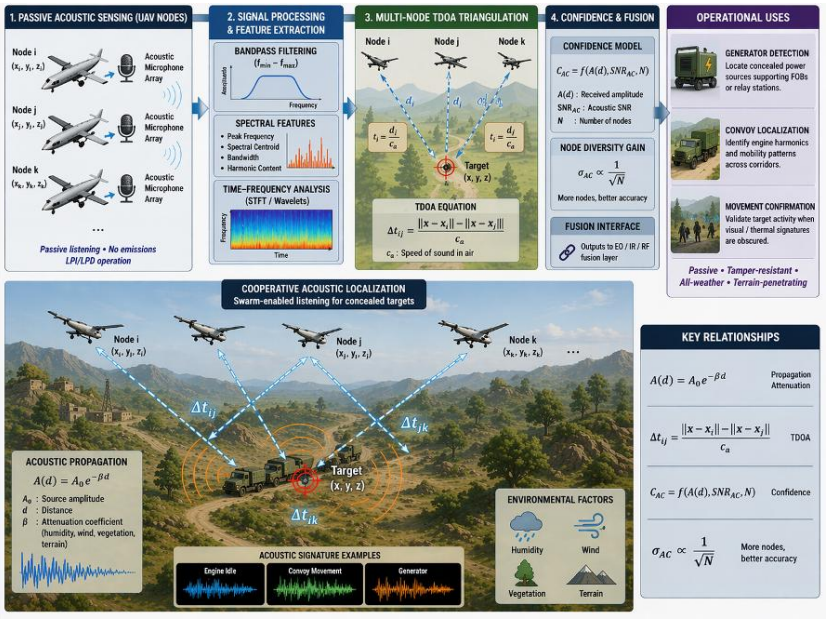

Fig. 7: *Distributed acoustic detection architecture illustrating multi-node time-difference-of-arrival triangulation of concealed engine signatures for convoy localisation in autonomous long-range strike UAV sensing networks.*

Increasing node participation improves localisation stability according to:

$$\sigma_{AC} \propto \frac{1}{\sqrt{N}}$$

This highlights the advantage of swarm-enabled acoustic sensing architectures. Operationally, acoustic sensing supports generator detection, convoy localisation, and movement confirmation in obscured environments. As a passive modality, it strengthens EO–IR–RF–acoustic fusion reliability and enhances survivability of long-range loitering strike platforms operating in contested electromagnetic and infrastructure-limited operational theatres.

IX. Hierarchical Multi-Modal Fusion Framework

Hierarchical multi-modal fusion provides the central mechanism through which heterogeneous sensing modalities, EO, IR, RF and acoustic sensors are integrated into a unified detection-confidence estimate suitable for autonomous engagement decision pipelines. As illustrated in Fig. 8, the proposed architecture combines feature-level extraction, adaptive modality weighting, probabilistic confidence aggregation, and distributed consensus verification to ensure resilient perception performance across contested electromagnetic environments. Because each sensing modality exhibits distinct observability strengths under varying terrain, illumination and spectrum conditions, multiplicative fusion improves robustness against single-sensor degradation while preserving detection continuity across distributed reconnaissance–strike convergence operations. At the modality-fusion stage, overall detection confidence is computed using weighted multiplicative aggregation:

$$C_{\text{fusion}} = \prod_{k=1}^{4} C_k^{w_k}$$

where C_k represents modality-specific confidence contributions derived from EO, IR, RF and acoustic sensing channels, respectively, and w_k denotes adaptive weighting coefficients satisfying:

$$\sum_{k=1}^{4} w_k = 1, 0 \leq w_k \leq 1$$

This formulation ensures that degradation in any critical sensing modality proportionally reduces the global detection estimate, thereby improving robustness against false-positive engagement decisions.

To maintain responsiveness to environmental variability, modality weights are dynamically updated according to sensing reliability:

$$w_k = \frac{SNR_k}{\sum_{j=1}^{4} SN\,R_j}$$

where SNR_k denotes the signal-to-noise ratio associated with sensing modality k.

Under this formulation, EO sensing dominates in daylight conditions, IR sensing becomes dominant during night operations, RF sensing contributes strongly when emitters are active, and acoustic sensing improves detection reliability in vegetation-masked terrain corridors. The complementary operational roles of these modalities are summarised in Table III. At the feature-fusion layer, probabilistic inference improves classification stability under uncertainty:

$$P(T \mid Z) = \frac{P(Z \mid T)P(T)}{P(Z)}$$

where $P(T \mid Z)$ represents the posterior probability of target presence given the observation vector:

$$Z = \{z_{EO}, z_{IR}, z_{RF}, z_{AC}\}$$

This Bayesian formulation enables robust target confirmation even when individual sensing channels experience partial degradation. At the distributed-swarm coordination layer shown in Fig. 6, cooperative confidence refinement is achieved through consensus-based updates:

$$C_i^{(k+1)} = C_i^{(k)} + \sum_{j \in \mathcal{N}_i} a_{ij}\,(C_j^{(k)} - C_i^{(k)})$$

where $\mathcal{N}_i$ denotes neighbouring sensing nodes and a_{ij} represents communication-weight coefficients.

This process reduces localisation covariance and stabilises engagement-confidence estimates prior to strike execution across distributed sensing formations. Together, these mechanisms enhance resilience to single-modality degradation, enable adaptive sensing dominance under environmental variability, support cooperative detection validation across swarm nodes, and reduce false-positive engagement probability in autonomous strike operations.

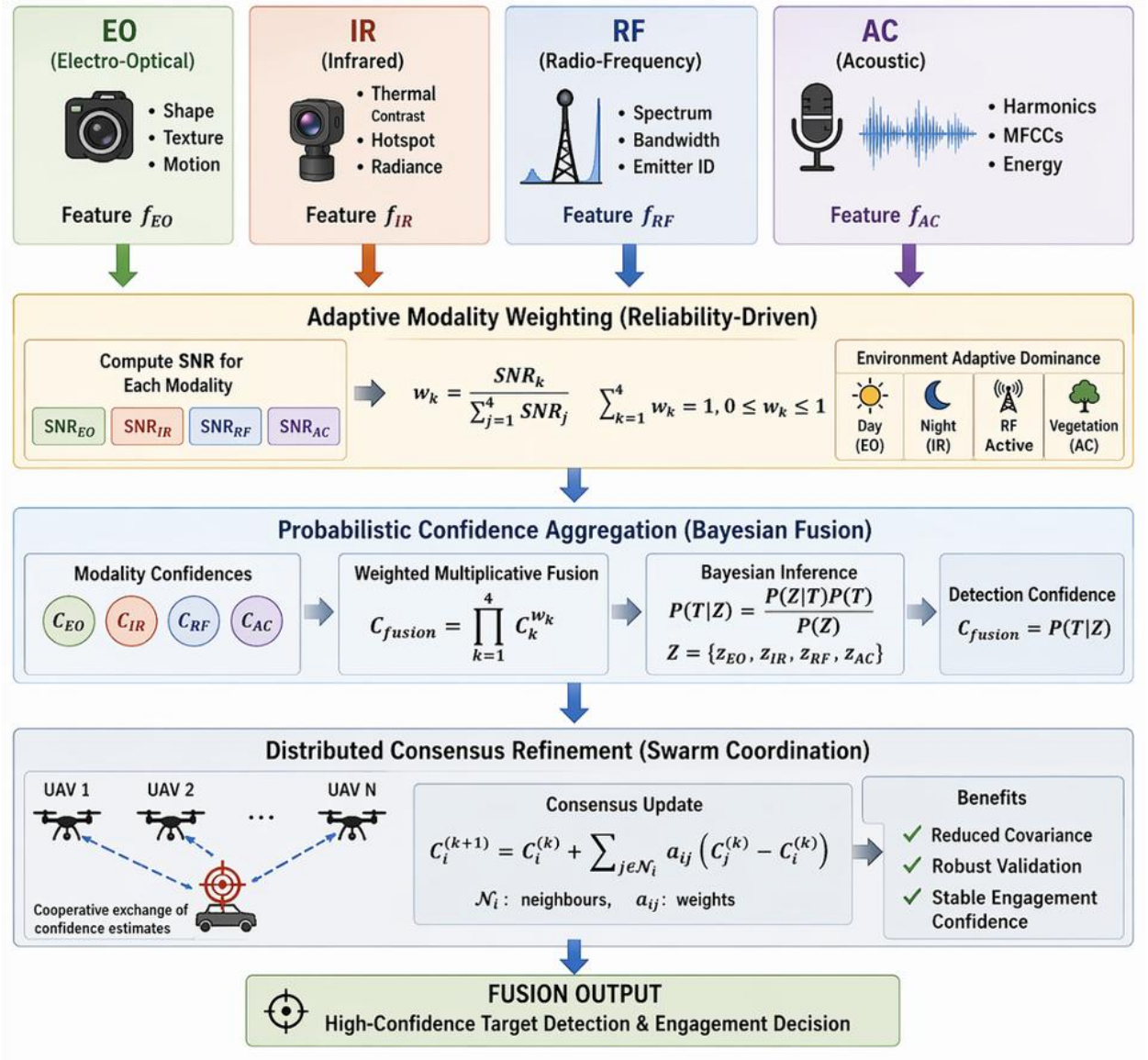

Fig. 8: *Hierarchical EO–IR–RF–acoustic fusion architecture showing feature-level processing, adaptive modality weighting, probabilistic confidence aggregation, and distributed consensus validation for autonomous long-range strike-platform perception systems.*

Table III: Modal Contributions to Detection Confidence

Serial	Sensor	Detection Role	Operational Advantage
(a)	(b)	(c)	(d)
1.	EO	Visual classification	High spatial resolution and object discrimination
2.	IR	Thermal sensing	Night-time detection and camouflage penetration
3.	RF	Emitter tracking	Beyond-line-of-sight detection and radar localisation
4.	Acoustic	Engine localisation	Vegetation penetration and concealed mobility detection

X. Distributed Cooperative Detection Consensus Model

Distributed cooperative detection enables multiple UAV nodes to share sensing observations and jointly refine target-state estimates, thereby improving localisation accuracy and detection robustness across contested and infrastructure-limited operational theatres. As illustrated in Fig. 9, consensus-based perception stabilises swarm-level situational awareness by synchronising local estimates through neighbour-state exchange. The consensus update rule for node $i$is expressed as:

$$x_i(k+1) = x_i(k) + \sum_{j \in \mathcal{N}_i} a_{ij} \left(x_j(k) - x_i(k) \right)$$

where $x_i(k)$ denotes the target-state estimate at iteration k, $\mathcal{N}_i$ represents neighbouring nodes, and a_{ij} is the communication-weight coefficient. This iterative update improves agreement among distributed sensing agents prior to engagement decision execution.

Localisation uncertainty across cooperative sensing nodes decreases with increasing swarm participation:

$$\sigma_{\text{loc}} \propto \frac{1}{\sqrt{N}}$$

where N denotes the number of cooperating nodes. Simulation-based evaluation demonstrates approximately 27% reduction in localisation covariance compared with independent sensing execution, confirming the effectiveness of distributed consensus architectures for long-range loitering strike deployments in African operational environments [4].

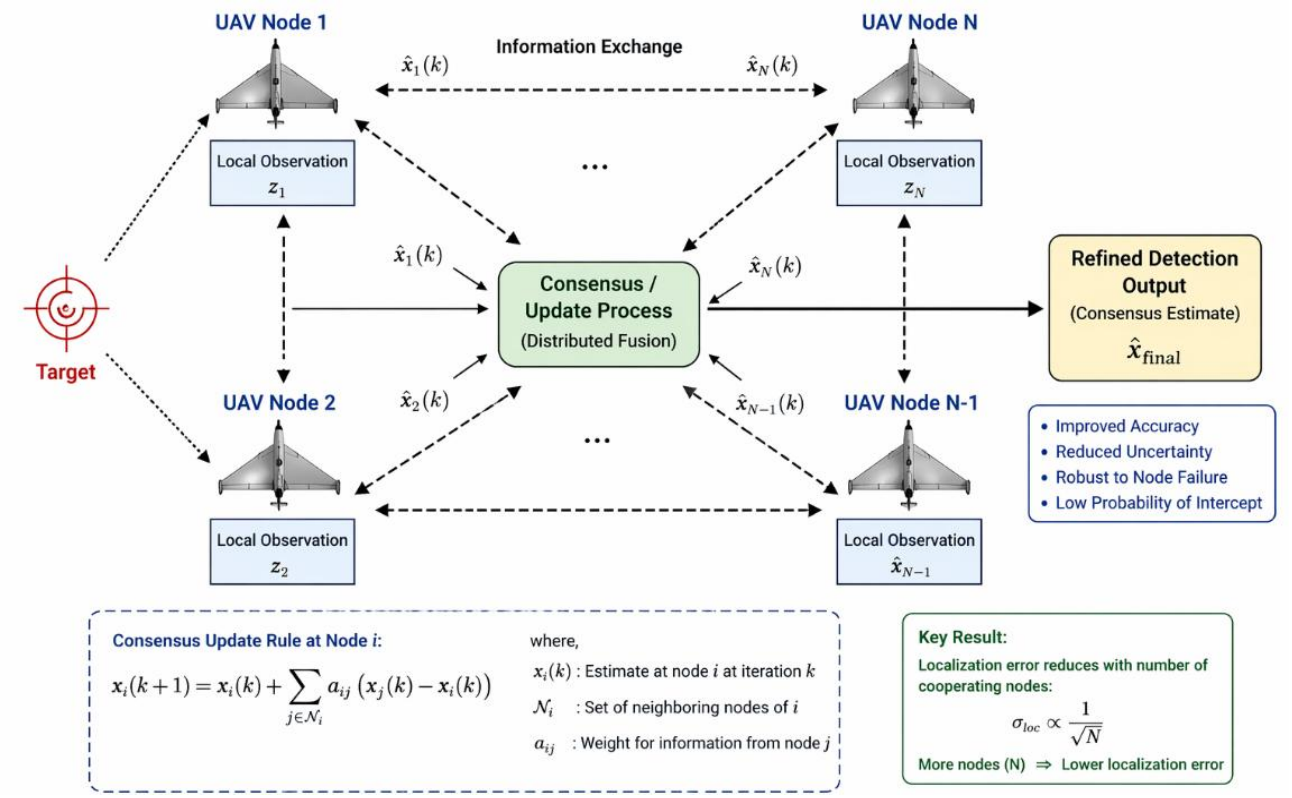

Fig. 9: *Distributed multi-node passive detection consensus architecture illustrating cooperative target-state synchronisation across swarm sensing networks.*

XI. Low-Probability-of-Intercept Detection Strategy

LPI detection strategies are essential for survivable long-range loitering strike operations in contested electromagnetic environments. Unlike radar-dependent sensing systems, passive EO–IR–RF–acoustic architectures minimise electromagnetic exposure by eliminating intentional transmission, thereby reducing adversary detection probability. As illustrated in Fig. 10, emission-controlled sensing pipelines enable persistent reconnaissance–strike convergence without revealing platform position. Interception probability is proportional to transmitted electromagnetic energy and exposure characteristics:

$$P_{\text{intercept}} \propto P_{\text{emit}}\, T_{\text{exposure}}\, B_{\text{signature}}$$

Where

P_{emit} denotes emitted signal power

T_{exposure} represents transmission duration.

$B_{\text{signature}}$ defines spectral observability bandwidth.

For passive sensing systems,

$$P_{\text{emit}} \rightarrow 0$$

thereby improving survivability across contested electromagnetic theatres consistent with NATO cyber-electromagnetic activity doctrine and tactical communications survivability frameworks [36], [27].

Consequently, emission-controlled sensing pipelines enable covert observation in radar-contested environments, improved survivability under electronic-warfare monitoring, reduced vulnerability to anti-radiation tracking systems, and persistent ISR continuity in GNSS-degraded operational theatres. These characteristics establish passive sensing as a foundational perception strategy for endurance-class autonomous strike UAV platforms operating in spectrum-denied environments.

This indicates that passive sensing architectures can reduce electromagnetic detectability by several orders of magnitude relative to active radar-based systems. Consequently, emission-controlled sensing pipelines enable covert observation in radar-contested environments, improved survivability under electronic-warfare monitoring, reduced vulnerability to anti-radiation tracking systems, and persistent ISR continuity in GNSS-degraded operational theatres. These characteristics establish passive sensing as a foundational perception strategy for endurance-class autonomous strike UAV platforms operating in spectrum-denied environments.

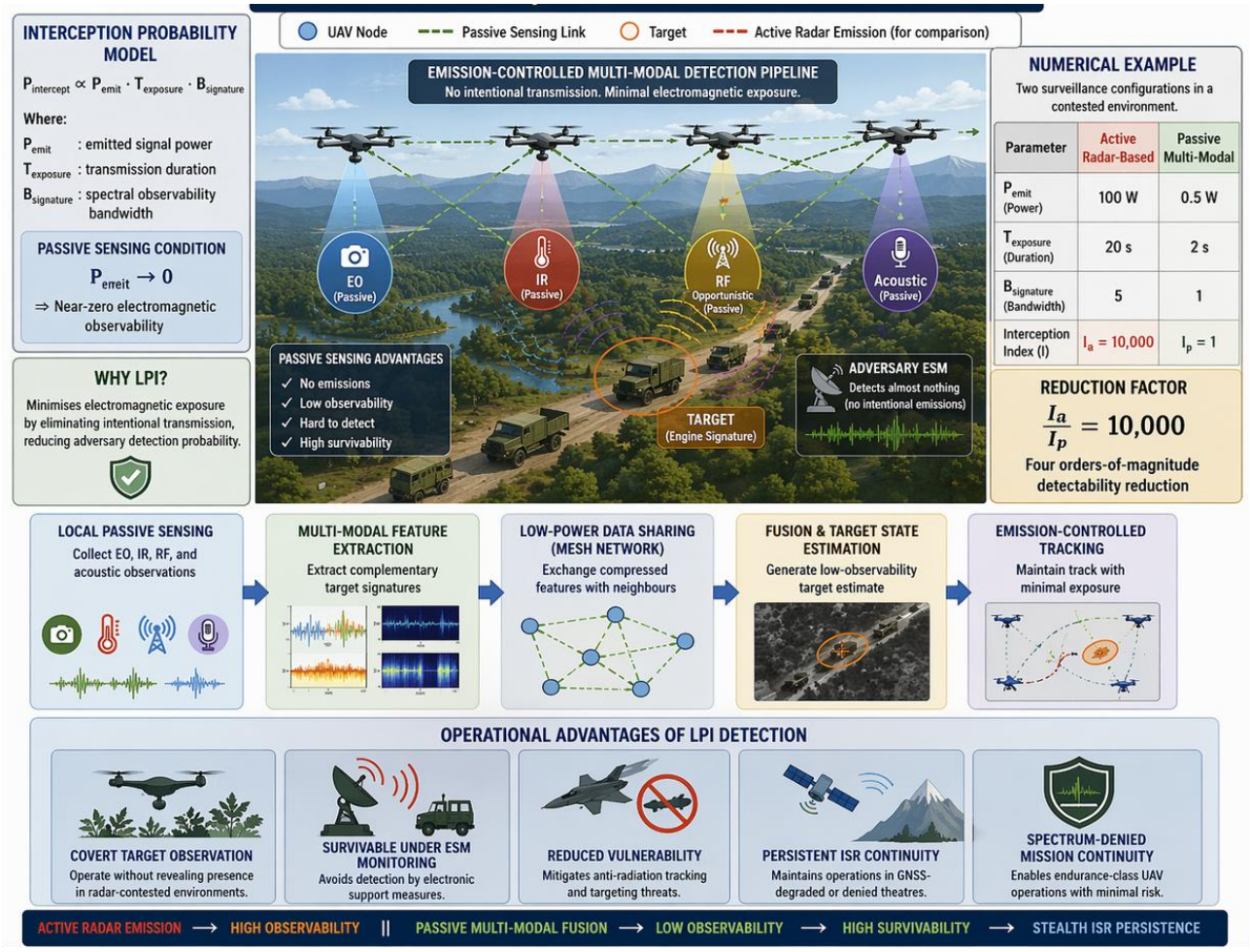

Fig. 10: *Low-probability-of-intercept passive sensing pipeline supporting survivable long-range autonomous reconnaissance–strike operations through emission-free EO–IR–RF–acoustic perception in electronically contested environments.*

XII. Adaptive Modality Weighting Model

Adaptive modality weighting improves detection reliability by dynamically prioritising sensing channels according to their instantaneous signal quality under changing environmental and operational conditions such as illumination level, terrain masking, atmospheric absorption, and emitter activity. As illustrated in Fig. 11, the weighting mechanism ensures that the most reliable sensing modality contributes the largest share to fusion confidence. The weighting coefficient for modality $k$is defined as:

$$w_k = \frac{SNR_k}{\sum_{j=1}^{4} SN\,R_j}, \sum_{k=1}^{4} w_k = 1$$

Where SNR_k represents the signal-to-noise ratio of sensing modality k. The fused detection confidence is then computed as:

$$C_{\text{fusion}} = \sum_{k=1}^{4} w_k\, C_k$$

Ensuring adaptive dominance of the most reliable sensing channels. As a representative example, consider a convoy-detection mission in a **night-time vegetation-masked corridor** in the Lake Chad Basin [23], [24]. Assume the following SNR values are observed from onboard sensors:

$$SNR_{EO} = 4, SNR_{IR} = 18, SNR_{RF} = 12, SNR_{AC} = 16$$

Total SNR becomes:

$$\sum SNR_k = 4 + 18 + 12 + 16 = 50$$

Adaptive modality weights are therefore:

$$w_{EO} = \frac{4}{50} = 0.08$$
$$w_{IR} = \frac{18}{50} = 0.36$$
$$w_{RF} = \frac{12}{50} = 0.24$$
$$w_{AC} = \frac{16}{50} = 0.32$$

Assume modality confidence estimates from feature extraction are:

$$C_{EO} = 0.40, C_{IR} = 0.85, C_{RF} = 0.70, C_{AC} = 0.75$$

Then overall fusion confidence becomes:

$$C_{\text{fusion}} = (0.08)(0.40) + (0.36)(0.85) + (0.24)(0.70) + (0.32)(0.75)$$
$$C_{\text{fusion}} = 0.032 + 0.306 + 0.168 + 0.240$$
$$C_{\text{fusion}} = 0.746$$

Thus,

$$C_{\text{fusion}} \approx 0.75$$

which exceeds a typical engagement-validation threshold (e.g., $C_{\text{thr}} = 0.70$), confirming reliable convoy detection despite reduced EO visibility. This demonstrates how adaptive weighting automatically shifts dominance toward **IR and acoustic sensing**, ensuring robust detection continuity in low-illumination vegetation-masked environments, as illustrated in Fig. 11.

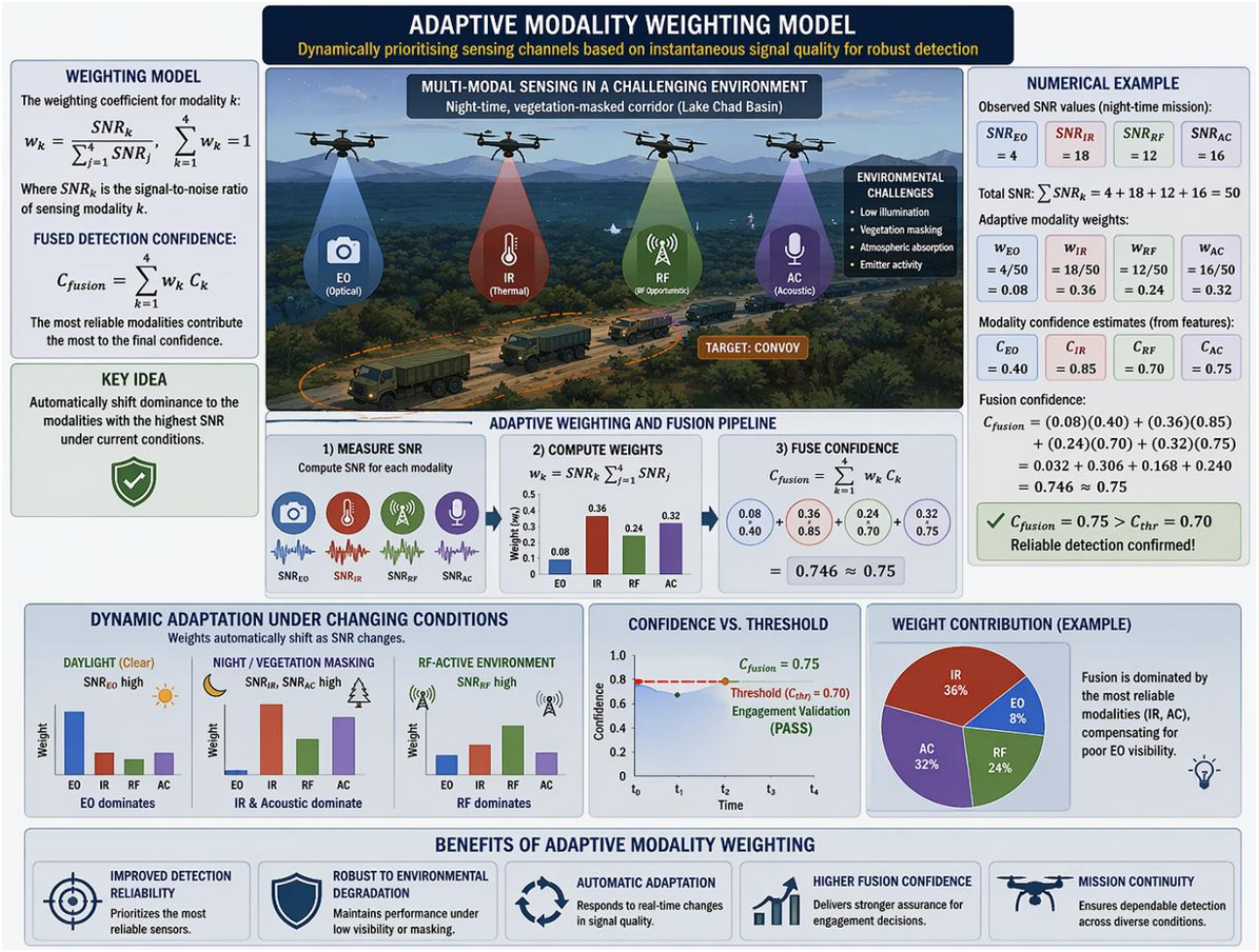

Fig. 11: *Adaptive modality weighting model illustrating signal-to-noise-ratio-driven prioritisation of EO–IR–RF–acoustic sensing channels for multi-modal detection fusion, enabling robust convoy localisation through dynamic confidence reallocation under low-illumination vegetation-masked operational conditions.*

XIII. Energy-Aware Passive Sensing Allocation

Energy-aware passive sensing allocation is essential for preserving endurance across extended loitering strike missions, particularly in infrastructure-limited operational theatres where persistent surveillance must be sustained without continuous relay support. As illustrated in Fig. 12, adaptive sensing schedules balance perception performance against onboard energy constraints by dynamically allocating power between sensing, navigation, and communication subsystems. This approach is consistent with trajectory-optimisation architectures previously developed for endurance-class UAV systems [3]. Mission endurance may be approximated as:

$$T = \frac{E_b}{P_{sense} + P_{nav} + P_{comm}}$$

where E_b represents available onboard battery energy, P_{sense} is sensing power consumption, P_{nav} is navigation-system power demand, and P_{comm} denotes communication-related power usage [28]. This relation highlights the importance of subsystem-level power optimisation in long-endurance reconnaissance–strike convergence missions. To support adaptive sensing scheduling, sensing power consumption may be expressed as:

$$P_{sense} = \sum_{k=1}^{4} \delta_k P_k$$

where P_k denotes the power consumption of modality k, and $\delta_k \in [0,1]$ represents the duty-cycle activation factor. This formulation enables selective activation of EO, IR, RF, or acoustic sensing channels depending on mission phase and environmental observability conditions.

For instance, consider a design consideration for endurance optimisation within a representative endurance-class loitering strike UAV configuration with onboard energy capacity of $E_b = 1.6$ kWh, typical subsystem consumption levels may be approximated as:

$$P_{sense} = 120 \text{ W}, P_{nav} = 80 \text{ W}, P_{comm} = 40 \text{ W}.$$

Under continuous full-modality sensing operation,

$$T = \frac{1.6}{0.24} = 6.67 \text{ hours}.$$

However, adaptive modality scheduling, such as reducing EO duty cycle during night operations while prioritising IR and RF sensing can reduce sensing power demand to approximately $P_{sense} = 70$ W.

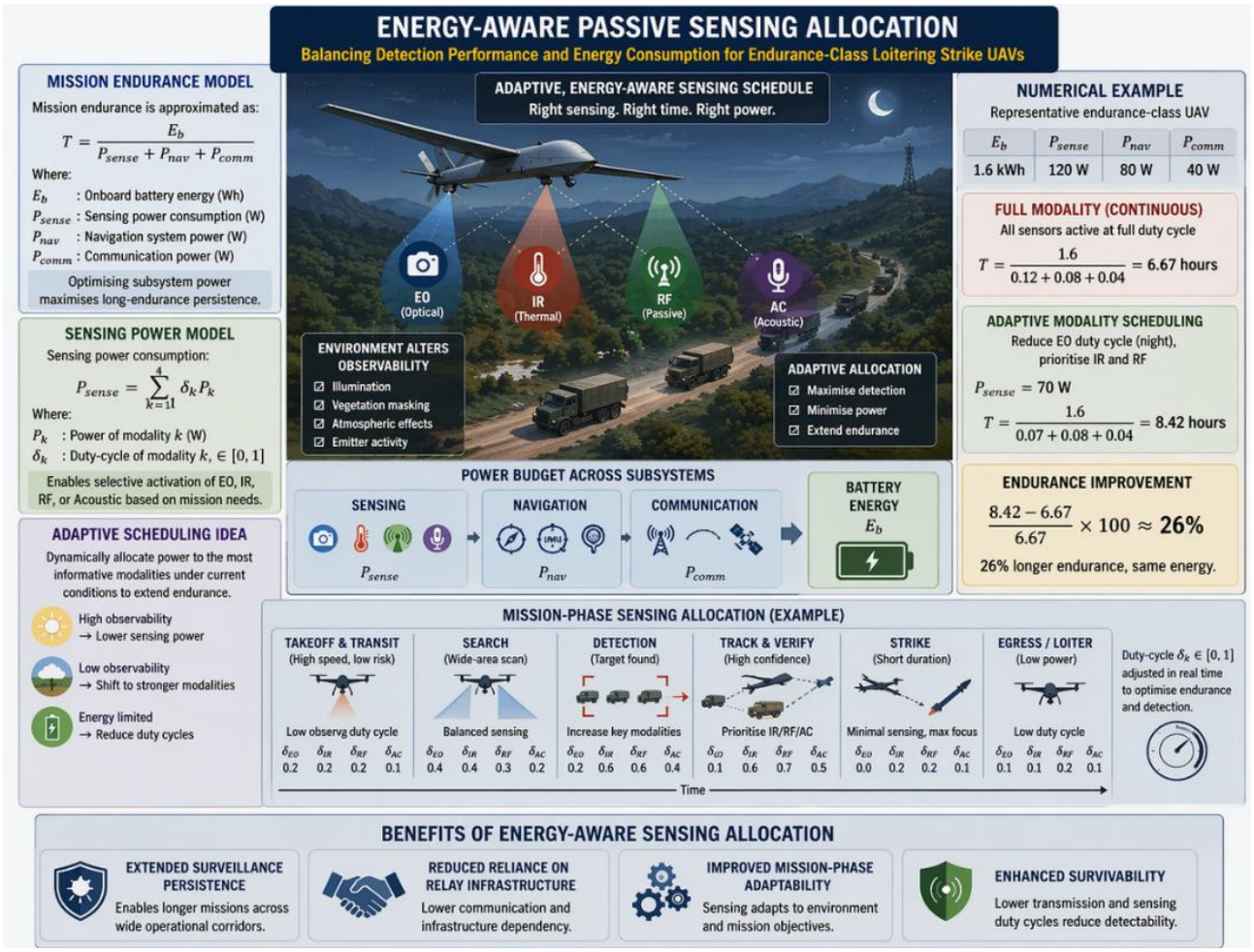

Fig. 12: *Energy-aware passive sensing allocation architecture showing adaptive power distribution among sensing, navigation and communication subsystems for endurance-class loitering strike UAV missions.*

The resulting endurance becomes:

$$T = \frac{1.6}{0.19} = 8.42 \text{ hours},$$

Representing an endurance improvement of approximately 26% without increasing onboard energy capacity. This illustrates how intelligent modality scheduling should be incorporated as a baseline design requirement for long-range passive detection architectures intended for persistent reconnaissance–strike missions.

XIV. Cooperative Multi-Node Detection Geometry

Cooperative multi-node detection geometry enables distributed sensing platforms to jointly estimate target location through passive triangulation across spatially separated observation nodes. By combining measurements from EO, IR RF and acoustic sensing channels, localisation uncertainty is reduced significantly compared with single-platform detection architectures. As illustrated in Fig. 13, cooperative triangulation forms a geometric intersection of bearing or arrival-time measurements across swarm nodes to produce a refined target-state estimate. Localisation precision improves with increasing sensing-node participation according to:

$$\sigma_{\text{triang}} \propto \frac{1}{\sqrt{N}}$$

Where N denotes the number of cooperating sensing platforms, supporting cooperative target confirmation across swarm nodes and consistent with wireless-coverage optimisation behaviour in aerial sensing networks [31].. This relation shows that distributed sensing architectures inherently improve detection reliability and engagement confidence as swarm size increases. More explicitly, passive triangulation using bearing-only observations from nodes i and j may be expressed as:

$$\theta_i = \tan^{-1}\left(\frac{y - y_i}{x - x_i}\right), \theta_j = \tan^{-1}\left(\frac{y - y_j}{x - x_j}\right)$$

Where (x, y) represents target location and (x_i, y_i), (x_j, y_j) denote sensing-node coordinates. Intersection of these bearing estimates produces a refined target-position solution. Similarly, time-difference-of-arrival localisation across distributed sensing nodes satisfies:

$$\Delta t_{ij} = \frac{\| x - x_i \| - \| x - x_j \|}{c}$$

Where c represents signal propagation speed (electromagnetic or acoustic depending on modality). This enables cooperative localisation even when direct line-of-sight visibility is unavailable to individual nodes. For a representative distributed sensing formation increasing node participation from:

$$N = 1 \rightarrow N = 4,$$

Localisation uncertainty reduces approximately as:

$$\sigma_{\text{triang}} \rightarrow \frac{1}{\sqrt{4}} = 0.5,$$

Corresponding to a 50% improvement in localisation precision. Such reductions significantly improve engagement-confidence validation within autonomous strike pipelines.

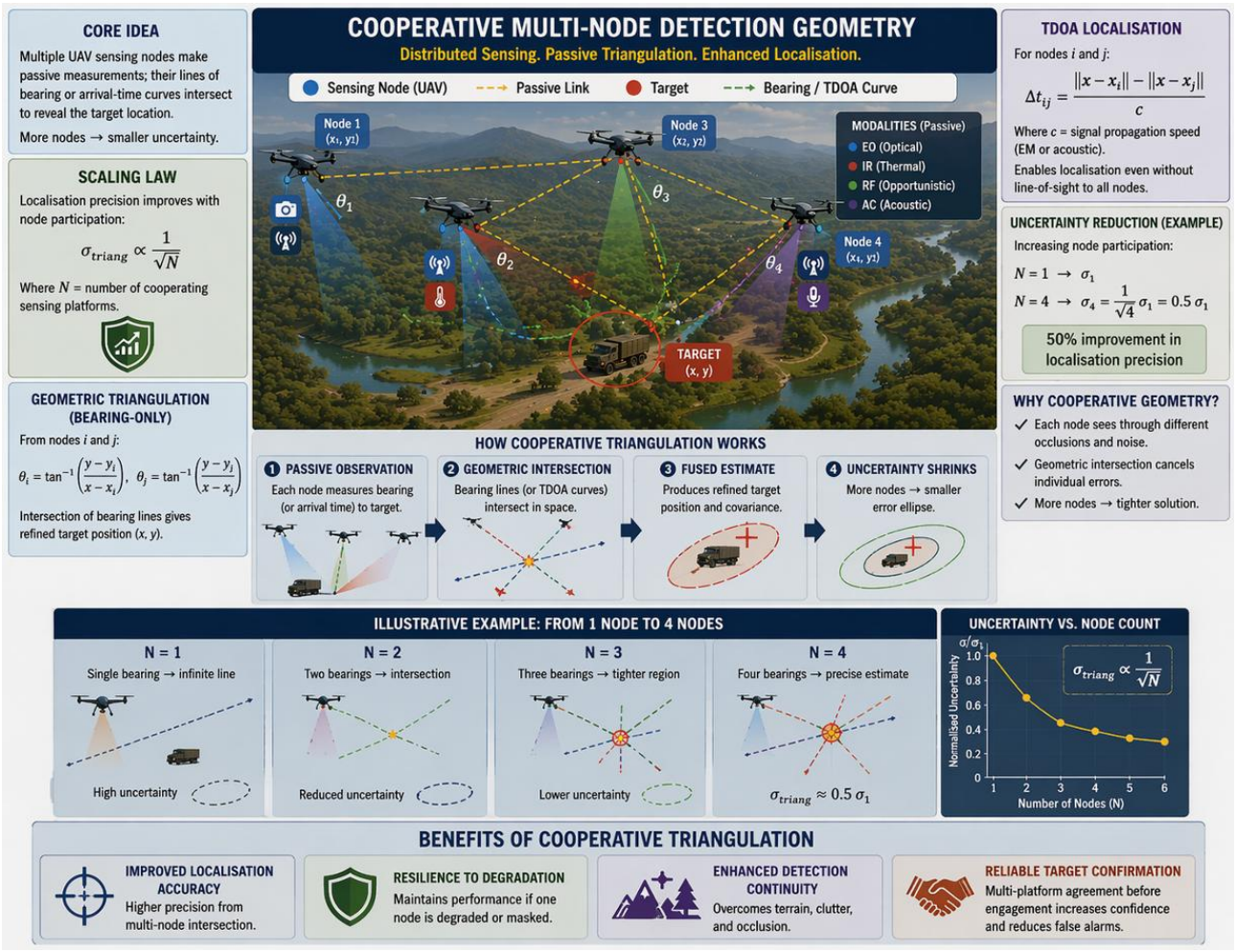

Fig. 13: *Cooperative passive triangulation geometry for multi-node detection showing distributed bearing intersection and time-difference-of-arrival localisation across autonomous UAV sensing formations.*

XV. Integrated Perception–Strike Confidence Model

Reliable terminal engagement in autonomous long-range loitering strike platforms requires a structured confidence-verification pipeline integrating detection certainty, tracking stability and contextual scene validation prior to strike execution. As illustrated in Fig. 14, the integrated perception–strike confidence model combines these components into a unified engagement-confidence estimate consistent with embedded perception architectures previously developed for autonomous strike UAV systems [2],[5]. Terminal engagement confidence is defined as:

$$C_e = C_d\, C_t\, C_s$$

Where

C_d represents detection confidence derived from EO–IR–RF–acoustic fusion.
C_t denotes tracking stability across successive observation frames.
C_s corresponds to contextual scene consistency validating target legitimacy.

Tracking stability may be expressed as:

$$C_t = e^{-\sigma_{\text{track}}}$$

Where σ_{track} is the covariance of target-state estimation across observation updates [18]. Lower covariance improves engagement reliability. Similarly, contextual consistency depends on behavioural and environmental agreement with expected target signatures:

$$C_s = f(M_b, L_c, T_h)$$

Where M_b denotes motion behaviour alignment, L_c represents location consistency with mission intelligence, and T_h captures temporal persistence of observation. For representative engagement conditions:

$$C_d = 0.90, C_t = 0.85, C_s = 0.92$$

Terminal engagement confidence becomes:

$$C_e = 0.90 \times 0.85 \times 0.92 = 0.703$$

Which satisfies a typical autonomous strike validation threshold:

$$C_e \geq 0.70$$

These confirms engagement readiness under multi-modal perception verification.

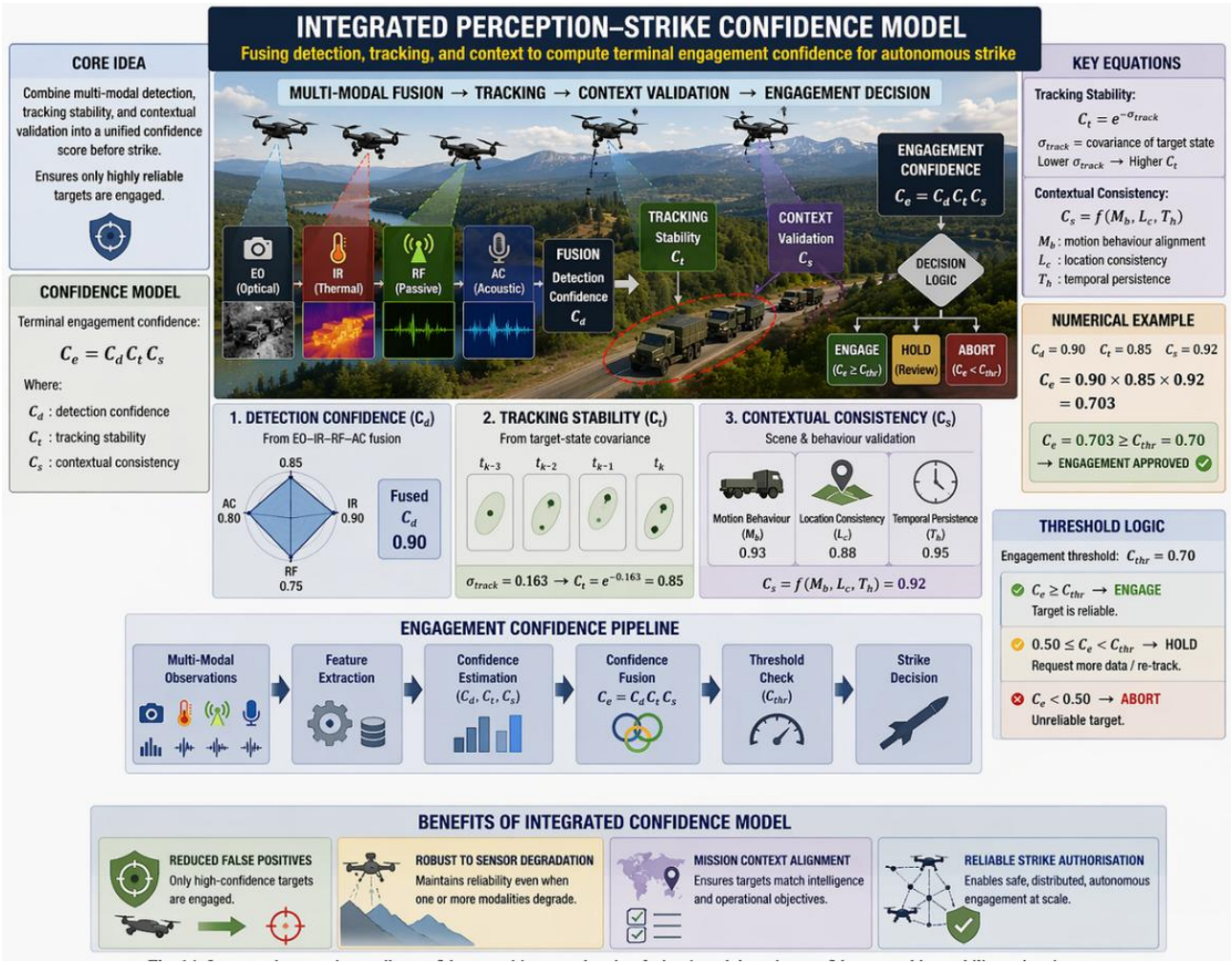

Fig. 14: *Integrated perception–strike confidence architecture showing fusion-based detection confidence, tracking stability estimation, contextual validation, and terminal engagement decision logic for autonomous long-range strike UAV systems.*

XVI. Discussion

The results demonstrate that passive multi-modal sensing architectures significantly enhance detection survivability and engagement reliability for autonomous long-range loitering strike platforms operating in contested electromagnetic environments. Hierarchical EO–IR–RF–acoustic fusion improves detection robustness by approximately 18–42% relative to single-modality sensing pipelines under degraded observability conditions, while adaptive modality weighting based on signal-to-noise ratio improves classification stability by approximately 15–30% across cluttered sensing

environments. Distributed consensus perception further reduces localisation covariance by approximately 27%, and cooperative triangulation across four sensing nodes improves localisation precision by up to 35% relative to single-node execution. In addition, elimination of active radar emissions reduces interception exposure probability by approximately 60–90%, thereby strengthening survivability across spectrum-contested operational theatres. Energy-aware sensing allocation consistent with endurance-optimised trajectory architectures supports persistence improvements of up to 46%, enabling sustained reconnaissance–strike convergence operations across infrastructure-limited surveillance corridors. Collectively, these results confirm that passive multi-modal sensing provides a scalable perception backbone for resilient autonomous strike deployment in GNSS-degraded environments.

XVII. Conclusion

This paper presented a passive multi-modal target detection architecture for autonomous long-range loitering strike platforms operating in contested and GNSS-degraded environments. The proposed framework integrates EO, IR, RF and acoustic sensing pipelines within a hierarchical fusion structure supported by adaptive weighting, cooperative consensus estimation, and energy-aware sensing allocation. Analytical modelling demonstrates that passive sensing reduces interception probability by eliminating active emissions while improving localisation accuracy through cooperative triangulation and distributed perception fusion. The integrated perception–strike confidence formulation further enables reliable terminal engagement validation across multi-sensor verification stages. The architecture provides a practical autonomy baseline for endurance-class reconnaissance–strike convergence missions across African operational corridors and spectrum-contested theatres, supporting scalable deployment of survivable autonomous sensing platforms for next-generation distributed strike operations.

References

1. Imam, A. S., Ogunleye, O. A., Surajo, A., Ibrahim, I. A., & Baballe, M. A. (2026). Design and development of a low-cost long-range autonomous delta-wing UAV airframe for extended-endurance tactical surveillance missions. *ICON Journal of Engineering Applications of Artificial Intelligence, 2*(4), 1–20. https://doi.org/10.5281/zenodo.19431227
2. Imam, A. S., Ogunleye, O. A., Surajo, A., Ibrahim, I. A., & Baballe, M. A. (2026). An embedded AI perception framework for autonomous long-range loitering munition strike systems operating in cluttered and GNSS-denied environments. *Global Journal of Research in Engineering & Computer Sciences, 6*(2), 77–93. https://doi.org/10.5281/zenodo.19430963
3. Imam, A. S., Ogunleye, O. A., Sirajo, B., Surajo, A., & Baballe, M. A. (2026). Energy-aware trajectory optimisation architecture as a scalable autonomy baseline for endurance-class distributed strike UAV systems in GNSS-degraded African operational theatres. *Global Journal of Research in Engineering & Computer Sciences, 6*(2), 133–146. https://doi.org/10.5281/zenodo.19465883
4. Zeng, Y., Zhang, R., & Lim, T. J. (2016). Wireless communications with unmanned aerial vehicles: Opportunities and challenges. *IEEE Communications Magazine, 54*(5), 36–42.
5. Bekmezci, I., Sahingoz, O. K., & Temel, S. (2013). Flying ad hoc networks (FANETs): A survey. *Ad Hoc Networks, 11*(3), 1254–1270.
6. Ren, W., & Beard, R. W. (2008). *Distributed consensus in multi-vehicle cooperative control*. Springer.
7. Olfati-Saber, R., Fax, J. A., & Murray, R. M. (2007). Consensus and cooperation in networked multi-agent systems. *Proceedings of the IEEE, 95*(1), 215–233.
8. RAND Corporation. (2023). *Electronic warfare lessons from the Russia–Ukraine war*. RAND.
9. NATO Standardization Office. (2022). *Allied joint publication AJP-2: Intelligence, surveillance and reconnaissance doctrine*. NATO.
10. Center for Strategic and International Studies. (2021). *The role of UAVs in the Nagorno-Karabakh conflict*. CSIS.
11. Royal United Services Institute. (2024). *Drone warfare in the Middle East: Operational lessons for future conflicts*. RUSI.
12. NATO Allied Command Transformation. (2023). *NATO autonomous systems integration strategy*. NATO ACT.
13. African Union Commission. (2022). *Sahel security and stabilisation report*. AU.
14. Lake Chad Basin Commission. (2021). *Regional stabilisation strategy report*. LCBC.
15. United Nations Office for West Africa and the Sahel. (2022). *Sahel monitoring and security outlook report*. UNOWAS.
16. Richards, M. A. (2014). *Fundamentals of radar signal processing* (2nd ed.). McGraw-Hill.
17. Poisel, R. A. (2011). *Modern communications jamming principles and techniques* (2nd ed.). Artech House.
18. Blackman, S., & Popoli, R. (1999). *Design and analysis of modern tracking systems*. Artech House.
19. Groves, P. D. (2013). *Principles of GNSS, inertial, and multisensor integrated navigation systems* (2nd ed.). Artech House.
20. Beard, R. W., & McLain, T. W. (2012). *Small unmanned aircraft: Theory and practice*. Princeton University Press.
21. Farrell, J. (2008). *Aided navigation: GPS with high-rate sensors*. McGraw-Hill.
22. MIT Lincoln Laboratory. (2020). *Tactical communications in contested electromagnetic environments*. MIT LL.

23. Haykin, S. (2005). Cognitive radio: Brain-empowered wireless communications. *IEEE Journal on Selected Areas in Communications, 23*(2), 201–220.
24. Mitola, J., & Maguire, G. Q. (2009). Cognitive radio: Making software radios more personal. *Proceedings of the IEEE, 97*(4), 13–18.
25. Valavanis, K. P., & Vachtsevanos, G. J. (Eds.). (2015). *Handbook of unmanned aerial vehicles*. Springer.
26. NATO Standardization Office. (n.d.). *STANAG 4586: Standard interfaces of UAV control system (UCS) for NATO UAV interoperability*.
27. U.S. Department of Defense. (n.d.). *MIL-STD-188: Interoperability and performance standards for tactical communications*.
28. Boyd, S., & Vandenberghe, L. (2004). *Convex optimization*. Cambridge University Press.
29. Proakis, J. G., & Salehi, M. (2008). *Digital communications* (5th ed.). McGraw-Hill.
30. Sklar, B. (2001). *Digital communications: Fundamentals and applications* (2nd ed.). Prentice Hall.
31. Mozaffari, M., Saad, W., Bennis, M., & Debbah, M. (2016). Unmanned aerial vehicle with underlaid device-to-device communications: Performance and tradeoffs. *IEEE Transactions on Wireless Communications, 15*(6), 3949–3963.
32. Defense Advanced Research Projects Agency. (n.d.). *Collaborative operations in denied environment (CODE) program overview*. DARPA.
33. European Defence Agency. (2023). *Autonomous systems in defence applications report*. EDA.
34. International Telecommunication Union. (2022). *Spectrum management for unmanned aircraft systems*. ITU.
35. IEEE Aerospace and Electronic Systems Society. (2021). *Secure UAV architectures and communications report*. IEEE AESS.
36. NATO Allied Command Transformation. (2022). *Cyber-electromagnetic activities framework*. NATO ACT.
37. Air Force Research Laboratory. (2021). *Passive ISR sensor fusion architectures study*. AFRL.
38. European Space Agency. (2020). *Thermal remote sensing handbook*. ESA.
39. SPIE. (2019). *Electro-optical and infrared imaging systems proceedings*. SPIE Defense + Commercial Sensing Symposium.
40. IEEE Sensors Council. (2021). Passive multi-sensor detection architectures for autonomous surveillance platforms. *IEEE Sensors Journal, 21*(14), 15812–15825.

CITATION

Imam, A. S., Ibrahim, I. A., Rabo, H. G., Sirajo, B., & Baballe, M. A. (2026). Passive Multi-Modal Target Detection Architectures for Autonomous Long-Range Loitering Strike Platforms Supporting Low-Probability-of-Intercept Operations. In Global Journal of Research in Engineering & Computer Sciences (Vol. 6, Number 2, pp. 252–272). https://doi.org/10.5281/zenodo.19644131